Correlation Lengths of the Wigner-Crystal Order in a Two-Dimensional Electron System at High Magnetic Fields

P. D. Ye,[1,2] L. W. Engel,[1] D. C. Tsui,[2] R. M. Lewis,[1,2] L. N. Pfeiffer,[3] and K. West[3]
[1]*National High Magnetic Field Laboratory, Tallahassee, Florida 32310*
[2]*Department of Electrical Engineering, Princeton University, Princeton, New Jersey 08544*
[3]*Bell Labs, Lucent Technologies, Murray Hill, New Jersey 07974*
(Received 4 April 2002; published 7 October 2002)

The insulator terminating the fractional quantum Hall series at low Landau level filling ν is generally taken to be a pinned Wigner crystal (WC), and exhibits a microwave resonance that is interpreted as a WC pinning mode. For a high quality sample at several densities, n, we find maxima in resonance peak frequency, f_{pk}, vs magnetic field, B. L, the correlation length of WC order, is calculated from f_{pk}. For each n, L vs ν tends at low ν toward a line with *positive intercept*; the fit is accurate over as much as a factor of 5 range of ν. The linear behavior is interpreted as due to B compressing the electron wave functions, to alter the effective electron-impurity interaction.

DOI: 10.1103/PhysRevLett.89.176802 PACS numbers: 73.43.Lp, 73.50.Mx, 75.40.Gb

The nature of a two-dimensional electron system (2DES) in high magnetic field (B) depends on the interactions of electrons with each other and with impurities, and on the overlap of individual electron wave functions. The size of an electron wave function, as measured by the magnetic length, $l_B = \sqrt{\hbar/eB}$, controls this overlap, and can also affect the electron-impurity interaction if the effective size or spacing of the impurities is comparable to l_B. In the high B limit, l_B vanishes, and electrons look like classical point particles. Without disorder, they are expected to form a Wigner crystal (WC), which is a triangular lattice stabilized by interelectron repulsion. Introduction of small amounts of disorder pins the WC, making it an insulator, and causing the crystalline order to have a finite correlation length, or domain size. The wave function overlap increases as B is decreased from the high B limit; its importance is characterized by l_B/a, where a is the WC lattice constant, or equivalently by the Landau filling factor $\nu = nh/eB = (4\pi/\sqrt{3})(l_B/a)^2$. At sufficiently high ν, calculated [1,2] for disorder-free systems to be around 1/7, the WC ground state is predicted to undergo a transition to the fractional quantum Hall effect (FQHE) [3] liquids.

Experimentally, 2DES are insulators from the maximum B accessed down at least to the high B edge of the 1/5 FQHE plateau [4,5]. Samples of sufficient quality to exhibit the 1/3 FQHE have a well-defined resonance [6–10] in the microwave spectrum of the high B insulating phase. The natural interpretation of the resonance is as a pinning mode of the WC, in which regions of WC oscillate within the impurity potential that pins them. The average (per electron) restoring force constant, K, on static displacement away from equilibrium positions determines the frequency of the resonance peak. This force constant is $K = m^*\omega_0^2$, which defines ω_0, the pinning frequency [11–13], with m^* the carrier effective mass. In the magnetic field, cyclotron motion mixes with the oscillation in the pinning potential for the resonating 2DES, resulting [11] in the observed resonance peak frequency $f_{pk} = \omega_0^2/2\pi\omega_c$, as long as the cyclotron frequency $\omega_c \gg \omega_0$, which must be the case for resonances in the frequency range of interest. In the classical, high B limit, in which l_B is much smaller than any feature of the disorder, and also small enough that wave function overlap of neighboring electrons can be neglected, ω_0 is constant in B, and $f_{pk} \propto 1/B$.

Correlation lengths of crystalline order can be calculated directly from f_{pk} and the elastic constants of the WC. Recent theories [14–16] identify the length directly relevant to f_{pk} as the Larkin length, L, over which displacements of equilibrium positions of electrons from perfect crystalline order reach the characteristic length of the electron-impurity interaction. In the classical, high B limit, the dependence of L on B has saturated, and L is a constant. Earlier theory [11–13] considered the particular case of a sinusoidal charge density wave, and so obtained f_{pk} in terms of a correlation length that we denote L_a, over which displacements of equilibrium positions from perfect crystalline order reach a.

The degree of WC order in 2DES has been considered previously. Time resolved photoluminescence [17] provided evidence for triangular crystalline ordering in the high B insulator. In double quantum wells, evidence for ordering came from commensurability effects [18]. In the context of a model [13], domain size has been estimated previously from early microwave [6], surface acoustic wave [19], and nonlinear I-V data [6,20].

This paper presents data on the microwave resonance for a high quality 2DES, surveyed over a wide range of B up to 20 T, and density, n, between 5.7 and 1.8×10^{10} cm^{-2}, to cover ν from 0.2 to 0.038. For all the n's we looked at, the resonance peak frequency, f_{pk}, vs B exhibits a maximum. Most likely because of higher quality in the present sample, such a maximum was not found in previous studies [6–9], in which f_{pk} vs B was increasing monotonically. We calculate L from f_{pk} and the

theoretical shear modulus of a WC of classical point particles, and find L in the range of 0.23 to 0.71 μm. Plots of L vs ν (with n fixed) tend toward a straight line, at low ν, with upward curvature developing at most n's as $\nu = 1/5$ is approached from below. We emphasize that the line has nonzero, positive intercept. The linear form for the L vs ν data is quantitatively convincing for the lowest few densities surveyed; at the lowest n there is a precise fit to the data over a factor of 5 in ν. The large ranges of linear fit for low n, extending to such low ν, suggest the linear behavior is an effect of the interplay of l_B and impurity correlation lengths. We interpret the upward curvature that sets in at higher ν as an effect of the correlations responsible for the FQHE.

The microwave methods used here are similar to those described earlier [8,9]. A metal film pattern (inset of Fig. 1) on the top of the sample forms a coplanar waveguide (CPW) transmission line consisting of a 45 μm wide center strip separated from side planes by slots of width $W = 30$ μm. The center conductor is driven and the two side conductors were grounded. The line couples capacitively to the 2DES. The geometry confines the microwave field mainly to the regions of 2DES under the slots.

The transmitted power was measured and normalized to unity for the case of vanishing σ_{xx}, obtained by depleting the 2DES with backgate voltage. The experiment is sensitive to σ_{xx} with wave vector $q \lesssim 2\pi/W$. We regard the 2DES as in the $q = 0$ limit in calculating the real part of diagonal conductivity, $\mathrm{Re}(\sigma_{xx})$. We obtained $\mathrm{Re}(\sigma_{xx})$ as $\mathrm{Re}(\sigma_{xx}) = W|\ln P|/2Z_0 d$, where P is the normalized transmitted power, $Z_0 = 50\ \Omega$, the $\sigma_{xx} = 0$ characteristic impedance, and $d = 28$ mm is the CPW length. This formula is valid in the high f, low loss limit, in the absence of reflections. Detailed simulation of the CPW with 2DES indicates this formula is correct to about $\pm 15\%$ under experimental conditions. The apparatus is typically 20 times more sensitive to $\mathrm{Re}(\sigma_{xx})$ than it is to $\mathrm{Im}(\sigma_{xx})$. The sample was in liquid of temperature $T \approx 50$ mK. Down to that T, resonance width for ν just below $1/5$ was sensitive to changes in bath T, indicating the 2DES was in reasonable equilibrium with the bath. The power was varied to ensure that the measurement was in a linear regime.

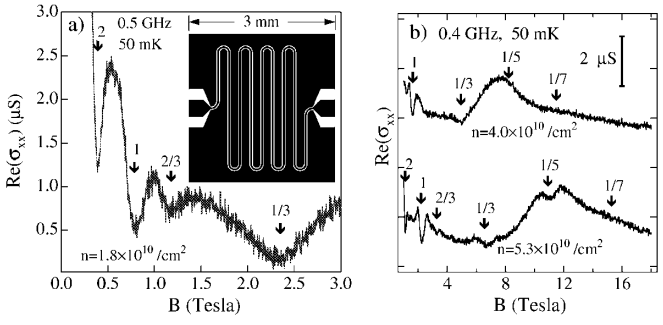

FIG. 1. Real part of diagonal conductivity $\mathrm{Re}(\sigma_{xx})$ vs magnetic field, B, for the sample at three different carrier densities n, filling factors ν marked by arrows. (a) $n = 1.8 \times 10^{10}$ cm^{-2}. Inset shows top view of transmission line, where black indicates metal film. (b) $n = 4.0 \times 10^{10}$ cm^{-2} and $n = 5.3 \times 10^{10}$ cm^{-2}.

The data were taken on a AlGaAs/GaAs heterojunction sample with as-cooled density (n) of 6.0×10^{10} cm^{-2} and 0.3 K mobility of 6×10^6 cm^2/V s. The sample was not illuminated, and its density was varied down to 1.8×10^{10} cm^{-2} by application of backgate voltage.

Figure 1 shows traces of $\mathrm{Re}(\sigma_{xx})$ vs B in the quantum Hall regime for three different n's, for $f = 0.4$ or 0.5 GHz. The 1/3 FQHE is present for all n's we survey; even the lowest n, 1.8×10^{10} cm^{-2}, in Fig. 1(a), exhibits well-defined FQH features, indicating the 2DES remains reasonably homogenous even at the large backgate bias required to produce that n. The 1/5 FQHE, however, is present only for larger n, as seen in Fig. 1(b), where a 1/5 FQHE minimum in $\mathrm{Re}(\sigma_{xx})$ vs B is present for $n \approx 5.3 \times 10^{10}$ cm^{-2} but absent for 4.0×10^{10} cm^{-2}. The traces of Fig. 1(b) show broad peaks beginning just above the 1/3 FQHE. These peaks are the manifestations in $\mathrm{Re}(\sigma_{xx})$ of the rapidly rising dc ρ_{xx} vs B [5,21], observed on increasing B beyond the 1/3 FQHE. The 1/5 FQHE minimum for $n \approx 4.0 \times 10^{10}$ cm^{-2} is superimposed on that peak.

Figure 2 shows typical resonance spectra, $\mathrm{Re}(\sigma_{xx})$ vs f, taken at various n and B. Spectra for several B are shown in Fig. 2(a) for $n = 1.8 \times 10^{10}$ cm^{-2} and in Fig. 2(b) for $n = 5.3 \times 10^{10}$ cm^{-2}. For ν just below 1/5, the resonance is present but comparatively broad; increasing B initially sharpens the peak and shifts it to higher f. At some n-dependent magnetic field, the resonance peak frequency, f_{pk}, goes through a maximum and begins to shift *downward* as B is increased further. The reduction of f_{pk} continues, and the resonance remains well developed, out to the maximum B measured. The maximum f_{pk} occurs around 10 T ($\nu = 0.074$) for $n = 1.8 \times 10^{10}$ cm^{-2} and around 15 T ($\nu = 0.146$) for $n = 5.3 \times 10^{10}$ cm^{-2}.

Figure 2(c) shows resonance spectra for fixed $B = 18$ T as n is varied. The resonances shift to higher f and broaden as n is decreased at fixed B for all B where the resonance is observed, as it did in other samples [6,9].

The behavior of the resonance vs T was similar to that of other samples [7,10]. At low $T \leq 100$ mK, increasing T broadens the resonance gradually, with little shift in f_{pk}, though resonance width can remain sensitive to the temperature of the bath down to 50 mK. f_{pk} appears to already be in a low T limit under the measuring conditions. The L values to be presented depend on f_{pk} but not on linewidth, and so may be regarded as in a low T limit.

Figure 3(a) shows f_{pk} vs ν for the various n's we studied. Each curve exhibits a maximum in f_{pk}, and the maxima shift generally to lower ν as n decreases. Full width at half-maximum linewidths, Δf, are plotted against the same axis in Fig. 3(b). These increase rapidly as the transition to the FQH liquid is approached. Around the ν where f_{pk} is maximal, the corresponding Δf curve for the same n shows a local minimum.

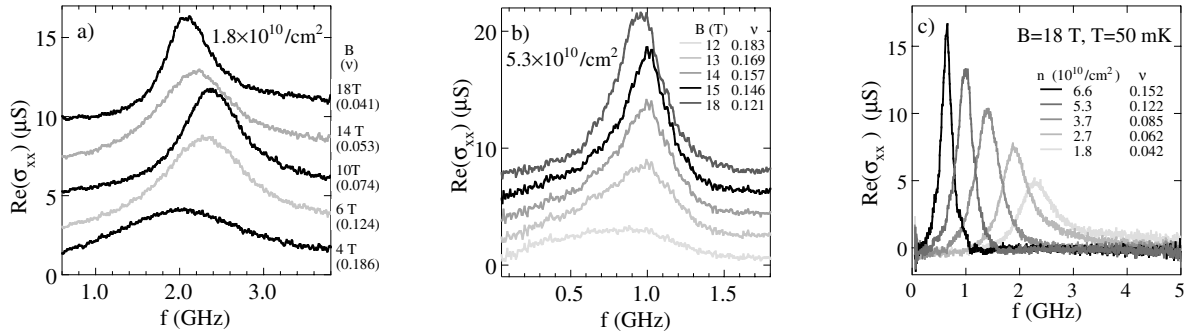

FIG. 2. Resonance spectra, real part of diagonal conductivity, $\mathrm{Re}(\sigma_{xx})$, vs frequency f. (a) Density $n = 1.8 \times 10^{10}$ cm^{-2}, various magnetic fields B. Successive curves offset in steps of 2.5 μS, for clarity; the 4 T curve is not offset. (b) Density $n = 5.3 \times 10^{10}$ cm^{-2}, various B. Successive curves offset in steps of 2.0 μS, for clarity. (c) Various n, for fixed $B = 18$ T.

The increasing f_{pk} vs ν (for fixed n) on the low ν side of the maxima may be viewed only as the approach to the classical regime in which $f_{pk} \propto \nu$ is expected. The observed increase is sublinear, and while the increase of f_{pk} with ν is a hint toward classical behavior, the fully classical, point particle picture is not applicable. Decreasing f_{pk} vs ν (increasing f_{pk} vs B), seen in the present data set on the high ν side of the maxima, and throughout previous data sets [7,8], has been interpreted in theories [14–16] based on interplay of l_B and some disorder correlation length, ξ, whose definition depends on the disorder model. The calculations, taken for weak disorder with $\xi \ll l_B$, give [14] $\mathrm{f_{pk}} \propto B$, or [15,16] $\mathrm{f_{pk}} \propto B^2$.

To more simply interpret the behavior of f_{pk} vs ν, we recast the f_{pk} data into domain size, L, using the elastic coefficients of the classical WC. L is the localization length of transverse phonons in the $B = 0$ crystal [16,22]. The angular pinning frequency $\omega_0 = c_t 2\pi/L$, where c_t is the $B = 0$ transverse phonon progagation velocity, $c_t = (\mu_t/nm^*)^{1/2}$. μ_t is the shear modulus. A WC of classical point particles [23] has shear modulus $\mu_{t,cl} = 0.245e^2n^{3/2}/4\pi\epsilon_0\epsilon$, where we take $\epsilon = 12.8$ as the GaAs host dielectric constant. ω_0 is gotten from f_{pk} data using the well-known formula [11] for $\omega_0 \ll \omega_c$ to take care of the effect of the Lorentz force on the dynamics, $\omega_0 = (2\pi f_{pk}\omega_c)^{1/2}$. With the classical shear modulus $\mu_{t,cl}$ we then get $L = (2\pi\mu_{t,cl}/neBf_{pk})^{1/2}$.

Figure 4 shows plots of L obtained this way vs ν for all the n's we measured. Figures 4(a) and 4(b) show the same data, with successive curves offset for clarity only in panel 4(a). Most striking are the data for the smallest n, 1.8×10^{10} cm^{-2}, which fit a straight line over the *entire range* of measurement of the resonance, over a factor of 5 in ν. The fit is accurate to within the instrumental errors in L, which we estimate as about ± 0.02 μm, propagating mainly from error in f_{pk}. The plots for all the other n tend to curve upwards for larger ν, as $1/5$ is approached. For the lower n's, the linear behavior holds over substantial ranges of ν and is quantitatively demonstrated.

The straight line regions of the L vs ν plots extend out to extremely low ν, so it is natural to interpret the linear behavior as an effect of electron-disorder interaction rather than interelectron wave function overlap. Particularly if it is due to interface roughness [14], the disorder potential can vary on extremely small length scales, down to about the lattice constant of GaAs. Such small disorder length scales would make the effects of electron-disorder interaction saturate less easily at high B than interelectron wave function overlap effects.

Because of the clear linear behavior for the lowest few n's, we fit the low ν tails of all the L vs ν plots to $L = \beta\nu + L_\infty$, where β and L_∞ are the fit parameters, and L_∞ is the domain size extrapolated to infinite B. The least squares fits are shown as heavy lines in Fig. 4(a), and extend over the points included in the fits. The inset to Fig. 4(b) shows the fit parameters. The curves appear irregular for larger n, and are more reliable for small n, where the linear ranges of L vs ν are substantial. For $n = 1.8 \times 10^{10}$ cm^{-2}, $L_\infty \approx 0.17$ μm $\approx 2.1a$. For the elastic model used to calculate L to be consistent with such $L \sim a$, we are assuming $\xi \ll a$, as proposed by Fertig [14]. In this case, $L_a \gg L$ is expected so that substantial crystalline positional order is still retained.

In the weak pinning energy limit, random pinning models [14–16] predict $L \sim n$, so that L increases when the WC is stiffer. $L \sim n$ may explain why the low n, low ν data of Fig. 4(b) group so closely when plotted against the Landau filling, which contains the density as well as the magnetic length, $\nu = 2\pi n l_B^2$. L_∞ vs n may give some insight into the pinning in the limit where electrons look similar to point particles. In the inset of Fig. 4(b),

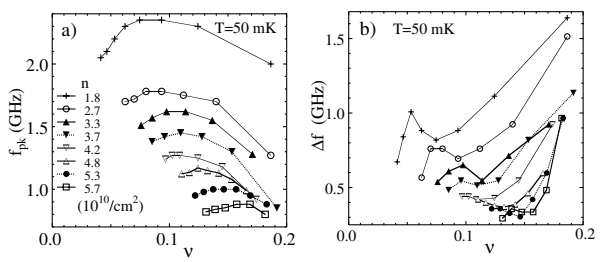

FIG. 3. (a) Peak frequency f_{pk} vs Landau filling ν for different carrier densities, n. (b) Full width at half-maximum linewidth, Δf, vs ν. Symbols are the same as in (a).

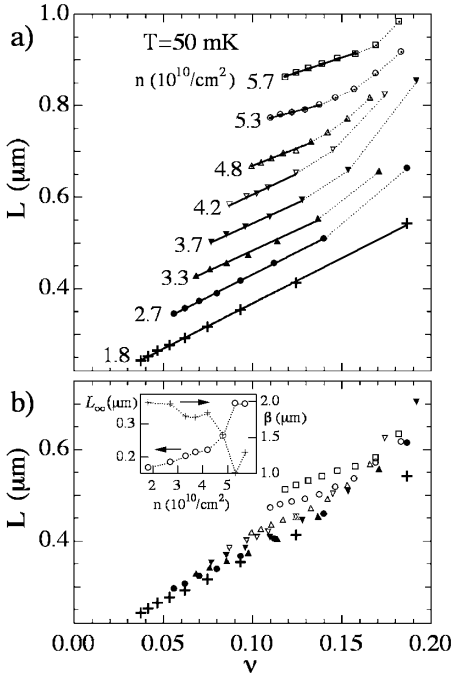

FIG. 4. Calculated domain sizes L vs Landau filling ν for various carrier densities n. (a) Successive curves are offset from each other by 0.05 μm. Curves are labeled with n (10^{10} cm^{-2}). Heavy lines are linear least squares fits to $L = \beta\nu + L_\infty$, extending over ranges of ν that were fit. (b) Same data as in (a), but not offset. Symbols for the n's are the same as in (a). Inset shows fit parameters, β and L_∞, vs n.

L_∞ vs n clearly increases, as expected for weak pinning. For $n \leq 4.2 \times 10^{10}$ cm^{-2}, L_∞ vs n is roughly linear, with a fit resulting in a slope of 2.3×10^{-22} m^3, and an intercept of 0.13 μm.

We interpret the upward curvature of L vs ν as $1/5$ is approached (except for $n = 1.8 \times 10^{10}$ cm^{-2}) as due to FQH-type correlations, which require interelectron overlap. One possibility is that, due to these correlations, μ_t decreases as $1/5$ is approached, as is predicted in a recent theory [24] of a WC of composite fermions. L presented in Fig. 4 is calculated using the classical shear modulus, $L \sim \mu_{t,cl}^{1/2}$, and would *overestimate* the true domain size, $\tilde{L}$, if the true shear modulus μ_t is less than $\mu_{t,cl}$. This would result in upward curvature of calculated L vs ν, even if the underlying $\tilde{L}$ vs ν were straight lines, such as the $n = 1.8 \times 10^{10}$ cm^{-2} plot in Fig. 4. We interpret the reduction in the curvature at low n as due to the suppression of the FQH-type correlations, owing to the increased importance at lower n of disorder relative to electron-electron interaction. This is consistent with Fig. 1(b), where the $1/5$ dip is suppressed at lower n.

In summary, systematic studies of the resonance for many n's show maxima in f_{pk} vs ν; these curves are greatly simplified on converting f_{pk} into L. L vs ν fits a line *with intercept* for low n and low ν, but curves upward as ν approaches $1/5$. The linear behavior is interpreted as an effect of interplay between electron wave functions and disorder features; the upward curvature is interpreted as an effect of FQH-type correlations, which may soften the WC.

The authors thank R. Chitra, H. Fertig, M. Fogler, and D. Huse for valuable discussions. Measurements were performed at the National High Magnetic Field Laboratory (NHMFL), which is supported by NSF Cooperative Agreement No. DMR-0084173 and by the State of Florida. This work is supported by the AFOSR, NSF, and NHMFL IHRP.

[1] Y. E. Lozovik and V. I. Yudson, JETP Lett. **22**, 11 (1975); P. K. Lam and S. M. Girvin, Phys. Rev. B **30**, 473 (1984); D. Levesque, J. J. Weis, and A. H. McDonald, Phys. Rev. B **30**, 1056 (1984); X. Zhu and S. G. Louie, Phys. Rev. B **52**, 5863 (1995).
[2] Kun Yang, F. D. M. Haldane, and E. H. Rezayi, Phys. Rev. B **64**, 081301 (2001).
[3] D. C. Tsui, H. L. Stormer, and A. C. Gossard, Phys. Rev. Lett. **48**, 1559 (1982).
[4] M. Shayegan, in *Perspectives in Quantum Hall Effects*, edited by S. Das Sarma and A. Pinczuk (Wiley, New York, 1996), p. 34.
[5] H. W. Jiang *et al.*, Phys. Rev. B **44**, 8107 (1991).
[6] D. C. Glattli *et al.*, Surf. Sci. **229**, 344 (1990); F. I. B. Williams *et al.*, Phys. Rev. Lett. **66**, 3285 (1991).
[7] L. W. Engel *et al.*, Solid State Commun. **104**, 167 (1997).
[8] C.-C. Li *et al.*, Phys. Rev. Lett. **79**, 1353 (1997).
[9] C.-C. Li *et al.*, Phys. Rev. B **61**, 10905 (2000).
[10] C.-C. Li *et al.*, J. Phys. (Paris) Colloq. **9**, Pr10-215 (1999).
[11] H. Fukuyama and P. A. Lee, Phys. Rev. B **17**, 535 (1978); **18**, 6245 (1978).
[12] B. G. A. Normand, P. B. Littlewood, and A. J. Millis, Phys. Rev. B **46**, 3920 (1992).
[13] A. J. Millis and P. B. Littlewood, Phys. Rev. B **50**, 17 632 (1994).
[14] H. A. Fertig, Phys. Rev. B **59**, 2120 (1999).
[15] R. Chitra, T. Giamarchi, and P. Le Doussal, Phys. Rev. Lett. **80**, 3827 (1998); Phys. Rev. B **65**, 035312 (2001).
[16] Michael M. Fogler and David A. Huse, Phys. Rev. B **62**, 7553 (2000).
[17] I. V. Kukushkin *et al.*, Phys. Rev. Lett. **72**, 3594 (1994); I. V. Kukushkin *et al.*, Phys. Rev. B **53**, 13 260 (1996).
[18] H. C. Manoharan *et al.*, Phys. Rev. Lett. **77**, 1813 (1996).
[19] M. A. Paalanen *et al.*, Phys. Rev. B **45**, 11 342 (1992).
[20] Y. P. Li *et al.*, Phys. Rev. Lett. **67**, 1630 (1992).
[21] T. Sajoto *et al.*, Phys. Rev. B **41**, 8449 (1990).
[22] In the $B = 0$ equivalent, the high B shear modulus and electron-impurity interactions are retained: Only the Lorentz force that mixes the elastic and cyclotron response is turned off.
[23] L. Bonsall and A. A. Maradudin, Phys. Rev. B **15**, 1959 (1977).
[24] R. Narevich, Ganpathy Murthy, and H. A. Fertig, Phys. Rev. B **64**, 245326 (2002).